Modeling the Evolution of the Dynamic Mechanical Properties of a Commercial Epoxy During Cure after Gelation

SINDEE L. SIMON,[1] GREGORY B. MCKENNA,[1] OLIVIER SINDT[2]

[1] Department of Chemical Engineering, Texas Tech University, Lubbock, TX 79409

[2] Currently at Shlumberger Doll Research, Ridgefield, CT 06877. Previously post-doctoral researcher under the direction of S.L.S. and G.B.M. at the University of Pittsburgh and the National Institute of Standards and Technology, respectively

Received 16 February 1999; accepted 29 October 1999

ABSTRACT: The cure kinetics for a commercial epoxy have been established and the influence of the degree of cure on the glass transition determined. Time-temperature and time-conversion superposition principles have been built into a model that successfully predicts the development of the viscoelastic properties of the epoxy during isothermal cure from gelation to after vitrification. © 2000 John Wiley & Sons, Inc.* J Appl Polym Sci 76: 495–508, 2000

Key words: cure; epoxy; thermoset; viscoelastic properties; shear modulus

INTRODUCTION

Understanding the cure of thermosetting materials is important to their application in the automotive, aerospace, and electronics industries. The isothermal time-temperature-transformation (TTT) cure diagram of Gillham[1,2] has provided an intellectual framework for understanding the behavior of these systems during cure, particularly the effects of gelation and vitrification on the cure kinetics and properties. Although the kinetics of the cure reaction(s) in cross-linking systems are very well-described, quantitative descriptions of the evolution of mechanical properties during cure are not well developed. Here we propose a methodology that combines the principles of time-temperature superposition, time-cross-link density superposition, and the rubbery elasticity of networks to accurately model the evolution of the viscoelastic properties during cure using limited experimental data. Such modeling may be expected to facilitate optimization of cure procedures in thermosetting systems, particularly for the reduction of residual stresses in, for example, composite materials.

The well-known principle of time-temperature superposition is based on the hypothesis that the mechanical response at short times (or high frequencies) is analogous to the response at low temperatures, and vice versa. The general validity of the concept is supported by the ability to satisfactorily reduce creep or stress relaxation data to form master curves.[3,4] The shift factors used to reduce viscoelastic data often follow the Williams-Landel-Ferry (WLF) equation[5] or the equivalent Vogel equation.[6] Arrhenius behavior has also been observed for some cross-linked systems with rigid backbones.[7–9]

The principle of time-cross-link density superposition is based on the assumption that the mechanical response of a loosely cross-linked material is shifted relative to that of a more highly cross-linked material. Plazek originally used time-cross-link density superposition to reduce

Correspondence to: S.L. Simon.

Journal of Applied Polymer Science, Vol. 76, 495–508 (2000)

creep curves in the terminal zone for natural rubber vulcanates.[10] In that work, the more loosely cross-linked materials were shifted horizontally to longer times due to the presence of longer relaxation times associated with the higher molecular weights between cross-link points. Other researchers have since applied the principle to the glass transition region. In this regime, the responses of the more loosely cross-linked materials are shifted to shorter times due to lower glass temperatures. For example, Lee and McKenna[11] applied time-cross-link density superposition to reduce stress relaxation data obtained during physical aging experiments for several epoxy systems having different molecular weights between cross-links. Plazek and Chay applied time-cure superposition to a model epoxy system to reduce the creep compliance obtained at different degrees of cure after accounting for the change in the glassy compliance; the curves were found to superpose at short times and deviated only in the terminal region of response.[12]

In addition to superposing the viscoelastic responses of materials of differing cross-link density, it is also necessary to model the effect of the cross-link density on the temperature dependence of the viscoelastic shift factors. In the early work by Suzuki and coworkers,[8] they found that the activation energy for the shift factors was independent of degree of cure for an epoxy resin. Similarly, Plazek and Chay found in their model epoxy system that the viscoelastic shift factors followed the same Vogel temperature dependence independent of degree of cure when the reference temperature was taken as the glass transition temperature. We note that such normalization of results to the glass transition temperature is common practice when parameters such as molecular weight, plasticizer content, or pressure are varied.[4]

In addition to incorporating the principles of time-temperature and time-cross-link density superposition in our model of the evolution of viscoelastic properties during cure, we also invoke the concept of rubber elasticity in the postgel material. We use the recursive approach of Miller and Macosko[13] to account for the conversion dependence of the rubbery modulus.

The paper is organized as follows. First we outline the methodology used to model the time, temperature, and conversion dependence of the shear modulus during cure. We then present the experimental methodology and the results of experimental studies. This is followed by the application of the model to a set of experimental conditions and comparison of model calculations with the relevant data. We end with some conclusions.

THERMO-VISCOELASTIC MODEL

Viscoelastic Response

The modulus of a thermosetting material with a given conversion is a function of time or frequency and temperature. The storage and loss moduli, as well as the stress relaxation modulus, can be approximated by a sum of Maxwell elements[4]:

$$G'(\omega) = G_r + [G_g - G_r]\sum_{i=1}^{n} g_i \frac{\omega^2\tau_i^2}{1 + \omega^2\tau_i^2} \quad (1)$$

$$G''(\omega) = [G_g - G_r]\sum_{i=1}^{n} g_i \frac{\omega\tau_i}{1 + \omega^2\tau_i^2} \quad (2)$$

$$G(t) = G_r + [G_g - G_r]\sum_{i=1}^{n} g_i e^{-(t/\tau_i)} \quad (3)$$

where G_g is the glassy value of the modulus that is not a strong function of temperature, G_r is the rubbery modulus that is a function of both temperature and conversion (or more precisely, cross-link density), t is time, and ω is radian frequency. τ_i is the i^{th} relaxation time and g_i is the weighting factor for the i^{th} relaxation time, such that $\Sigma g_i = 1.0$. The relaxation times τ_i are functions of temperature as well as conversion (or cross-link density).

Effects of Temperature and Conversion on G_r

The effects of temperature and conversion on the rubbery modulus are given by the theory of rubber elasticity:

$$G_r(T, x) = A\nu RT = \frac{G_{r,\text{ref}}T\nu}{T_{\text{ref}}\nu_{\text{ref}}} \quad (4)$$

where x is conversion, A is a prefactor, ν is the effective concentration of network chains, and $G_{r,\text{ref}}$ refers to the value of the rubbery modulus at the reference conditions, T_{ref} and ν_{ref}, where ν_{ref} is determined at the reference conversion, x_{ref}. The effective concentration of network chains can be related to conversion using the recursive

approach of Miller and Macosko.[13] For a difunctional epoxy and a tetrafunctional cross-linker, ν is given by:

$$\nu = (1 - P)^4 + \tfrac{1}{2}P(1 - P)^3 \quad (5)$$

with P, the probability that a given arm of the cross-linker is not connected to the infinite network, given by:

$$P = \left(\frac{1}{rx^2} - \frac{3}{4}\right)^{1/2} - \frac{1}{2} \quad (6)$$

where r is the stoichiometric ratio of the limiting reagent to the excess reagent ($r < 1.0$) and x is the conversion.

Temperature and Conversion Shift Factors

The effects of temperature and conversion on the relaxation time are accounted for by applying the principles of time-temperature and time-cross-link density superposition. We use a temperature shift factor, a_T, to account for the temperature dependence of each relaxation time τ_i:

$$\tau_i(T) = a_T\tau_i(T_{\text{ref}}) \quad (7)$$

Because the material is assumed to be thermorheologically simple, all relaxation times are shifted in the same way. Similarly, a cross-link shift factor, a_x, accounts for the cross-link-density dependence of the relaxation time:

$$\tau_i(T_g) = a_x\tau_i(T_g(x_{\text{ref}})) \quad (8)$$

where $T_g(x_{\text{ref}})$ is the glass transition temperature at the reference conversion (reference cross-link density). The temperature shift factor is expected to follow a generalized Vogel equation,[6] because the Vogel equation is capable of describing both WLF behavior[5] and Arrhenius behavior (when $T_\infty = 0$ K):

$$\log a_T = \log \frac{\tau_i(T)}{\tau_i(T_{\text{ref}})} = \frac{C}{T - T_\infty} - \frac{C}{T_{\text{ref}} - T_\infty} \quad (9)$$

In eq. (9), T_∞ is a function of conversion (T_g) if the WLF equation applies: $T_\infty = T_g - C_2$, where C_2 is a constant (51.6 in the "universal" WLF equation[5]).

We postulate that the cross-link (conversion) shift factor has a similar form independent of cross-link density if the reference temperature is taken as T_g based on the work cited in the introduction[4,7,11,12]:

$$\log a_x = \log \frac{\tau_i(T_g(x))}{\tau_i(T_g(x_{\text{ref}}))} = -\left(\frac{C}{T_g(x) - T_\infty} - \frac{C}{T_g(x_{\text{ref}}) - T_\infty}\right) \quad (10)$$

where C and T_∞ are constants as in eq. (9) (with T_∞ depending on T_g if the WLF equation applies), $T_g(x)$ emphasizes that T_g is a function of conversion, and $T_g(x_{\text{ref}})$ is T_g at the reference conversion. Combining these equations gives the shift factor as a function of both temperature and cross-link density (or T_g):

$$\log a_{T,x} = \log \frac{\tau_i(T,\ T_g(x))}{\tau_i(T_{\text{ref}},\ T_g(x_{\text{ref}}))} = \left(\frac{C}{T - T_\infty} - \frac{C}{T_{\text{ref}} - T_\infty}\right) - \left(\frac{C}{T_g(x) - T_\infty} - \frac{C}{T_g(x_{\text{ref}}) - T_\infty}\right) \quad (11)$$

It is noted that T_{ref} and $T_g(x_{\text{ref}})$ need not be the same. T_{ref} is the reference temperature for the viscoelastic master curve of the fully cured material, whereas $T_g(x_{\text{ref}})$ is the glass temperature of the material at the reference conversion, x_{ref}. If, however, x_{ref} is taken to be 1.0 and $T_{\text{ref}} = T_g(x_{\text{ref}})$, then eq. (11) can be simplified:

$$\log a_{T,x} = \log \frac{\tau_i(T,\ T_g(x))}{\tau_i(T_{\text{ref}},\ \mathrm{T_g(x_{ref})})} = \frac{C}{T - T_\infty} - \frac{C}{T_g(x) - T_\infty} \quad (12)$$

In order to describe the shift factor in terms of conversion and temperature rather than in terms of T_g and temperature, we need to relate T_g to conversion. For many thermosetting systems, there is a unique relationship between T_g and conversion,[14–16] which can often be described by the empirical DeBenedetto[17] equation:

$$\frac{T_g - T_{go}}{T_{g\infty} - T_{go}} = \frac{\lambda x}{1 - (1 - \lambda)x} \quad (13)$$

where T_{go} is the T_g of the monomer, $T_{g\infty}$ is the T_g of the fully cured material ($x = 1.0$), and λ is a material constant.

Using eq. (4) through (6) and (12) and (13), the moduli as a function of temperature and conversion can be calculated using the principles of time-temperature and time-conversion (time-cross-link density) superposition:

$$G'(\omega, T, x) = G_r(T, x) + [G_g - G_r(T, x)]\sum_{i=1}^{n} g_i \frac{\omega^2 a_{T,x}^2 \tau_i^2}{1 + \omega^2 a_{T,x}^2 \tau_i^2} \quad (14)$$

$$G''(\omega, T, x) = [G_g - G_r(T, x)] \times \sum_{i=1}^{n} g_i \frac{\omega a_{T,x} \tau_i}{1 + \omega^2 a_{T,x}^2 \tau_i^2} \quad (15)$$

$$G(t, T, x) = G_r(T, x) + [G_g - G_r(T, x)]\sum_{i=1}^{n} g_i e^{-(t/a_{T,x}\tau_i)} \quad (16)$$

Invoking a model of the cure kinetics further allows the viscoelastic properties to be calculated as a function of time during cure and compared to experimental data. The model of the cure kinetics used in this work is discussed in the results section along with the experimental data.

EXPERIMENTAL METHODS

Material

The material investigated is a commercial toughened epoxy resin, Hexcel 8551-7, supplied by Hexcel Corporation (Dublin, CA). According to the resin manufacturer, there is some percentage of polysulfone in the resin that phase separates during cure—an important phenomenon for toughening of thermoset resins used in composite materials. Although this commercial resin system is complex, and hence, might not be considered ideal for our investigation, our ability to model its behavior demonstrates the utility of the methodology developed.

Viscoelastic Studies of the Fully Cured Material

To obtain the viscoelastic behavior of the fully cured epoxy resin, material was cured at 180°C for 5 h in a test tube approximately 1 cm in diameter and 10 cm in length. Full conversion was expected based on the kinetic model (see later). The temperature was then decreased from 180°C to ambient temperature in 2 h, in the oven. In order to avoid the formation of cracks in the sample during the cure and the cooling, the inner surface of the test tube was sprayed with silicon oil before filling the tube with the resin. Once the sample was cured the tube was broken and the epoxy removed. Then, the diameter and length of the sample were adjusted using a lathe to approximately 6.5 mm and 25 mm, respectively.

The viscoelastic measurements were made in shear using a Rheometric Scientific, Inc. (Piscataway, NJ) ARES instrument at temperatures ranging from 140°C to 180°C. Experiments were performed to obtain both stress relaxation modulus, $G(t)$, and the dynamic moduli, $G'(\omega)$ and $G''(\omega)$. The temperature control was stable as measured to ± 0.05°C. Rod fixtures were used to hold the sample in place and measure its properties. Once placed into the apparatus, the length of the sample was approximately 25 mm at 20°C (measured to ± 0.001 mm by the apparatus). Prior to making a measurement, the sample was held at 170°C (above the maximum glass temperature measured by differential scanning calorimetry [DSC]) for 1 h in order to erase any previous thermal history of the sample. Then, for each temperature studied, the sample was held at the testing temperature for 1 h (3600 s) without any applied load. Subsequently, the stress relaxation test was performed for a time equal to 10% of the previous time (360 s) following Struik's protocol[18] to insure that negligible physical aging occurred during the measurements. After the stress relaxation test was performed, a frequency sweep was performed at the same temperature from 1 to 30 rad/s. After the stress relaxation experiment and frequency sweeps were made, the temperature was set again to 170°C, and a new test was run following the thermal scheme described above. During both the stress relaxation and dynamic mechanical experiments, the shear deformation applied was 0.0002, which assures that the experiments were carried out in the linear viscoelastic domain.

Studies of Viscoelastic Properties During Cure

The Rheometric Scientific ARES instrument was also used to measure the dynamic mechanical properties, $G'(\omega)$ and $G''(\omega)$, during isothermal

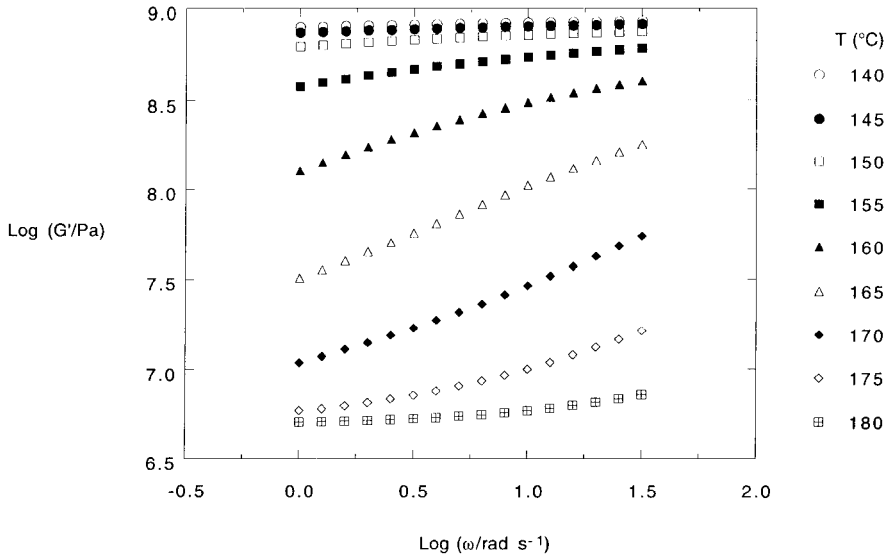

Figure 1 Double logarithmic representation of the storage modulus vs frequency for the fully cured material. The temperatures are as indicated.

cure. Measurements were made in shear using a parallel plate geometry at 1 Hz. The diameters of the platens were 8 mm, and the thicknesses of the samples were between 2 and 4 mm (determined to ±0.001 mm). The samples were loaded at room temperature and then heated at a rate of 5°C/min to the desired cure temperature, between 145°C and 180°C. Measurements were made for approximately 2 h at the isothermal temperature as the material cured. Again, the maximum shear strain used was 0.0002 to assure linearity of the response.

DSC Studies of the Cure Kinetics

The cure kinetics of the resin were studied using a Perkin Elmer, LLC (Norwalk, CT) DSC-7 DSC. This information is needed to transform the viscoelastic calculations made as a function of conversion to a function of time of cure in order to compare the calculations with the experimental data. DSC measurements were made on resin encapsulated in nonhermetic pans. The glass transition temperature of the uncured material (T_{go}) and the total heat of reaction (ΔH_T) were obtained by scanning uncured samples from −40°C to 300°C at a heating rate of 10°C/min. Partially cured material was prepared by curing in the DSC at the desired cure temperature, ranging from 120°C to 160°C, for times up to 10 h. After curing for a preselected time, the sample was cooled to −40°C at a rate of 20°C/min. Subsequently, the sample was scanned during heating at 10°C/min. From this scan, T_g and the residual heat of reaction, ΔH_{res}, were obtained. The glass transition temperature is taken to be the temperature of the midpoint of the step change in the heat capacity. The conversion was calculated from the residual heat:

$$x = 1 - \frac{\Delta H_{\text{res}}}{\Delta H_T} \tag{17}$$

When the sample vitrified during cure, the resulting physical aging peak observed near T_g makes it difficult to accurately measure the residual heat of reaction. In these cases, the sample was cooled to −40°C after the maximum in the annealing peak was observed and then rescanned at 10°C/min to 300°C. This procedure removed the annealing peak on the rescan thereby allowing the residual heat of reaction to be accurately measured.

RESULTS

Dynamic Mechanical Response and Stress Relaxation for the Fully Cured Material

The frequency-dependent storage and loss moduli $G'(\omega)$ and $G''(\omega)$ for the fully cured material are shown in Figures 1 and 2 for temperatures rang-

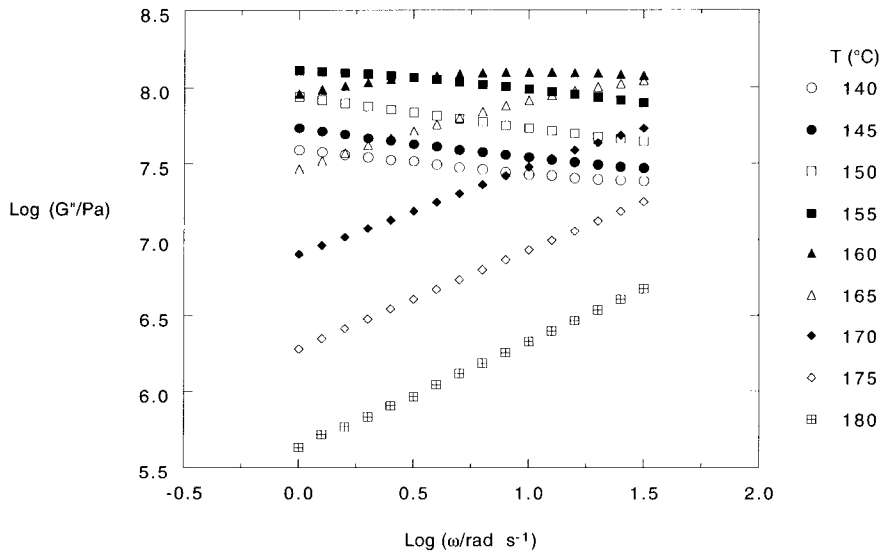

Figure 2 Double logarithmic representation of the loss modulus vs frequency for the fully cured material. The temperatures are as indicated.

ing from 140°C to 180°C. Experimental data were obtained every 2.5°C but only some of the temperatures are shown for purposes of clarity. At the lowest temperatures, the storage modulus shows glassy behavior with a modulus of approximately 860 MPa. As the testing temperature is increased through the glass transition temperature, the storage modulus drops and the loss modulus goes through a maximum. At the highest temperatures, the rubbery modulus is found to be approximately 4.6 MPa.

The master curves for the dynamic mechanical data are shown in Figure 3. The master curves were constructed by time-temperature superposition using 160°C as the reference temperature. No vertical shifts were needed. A master curve for

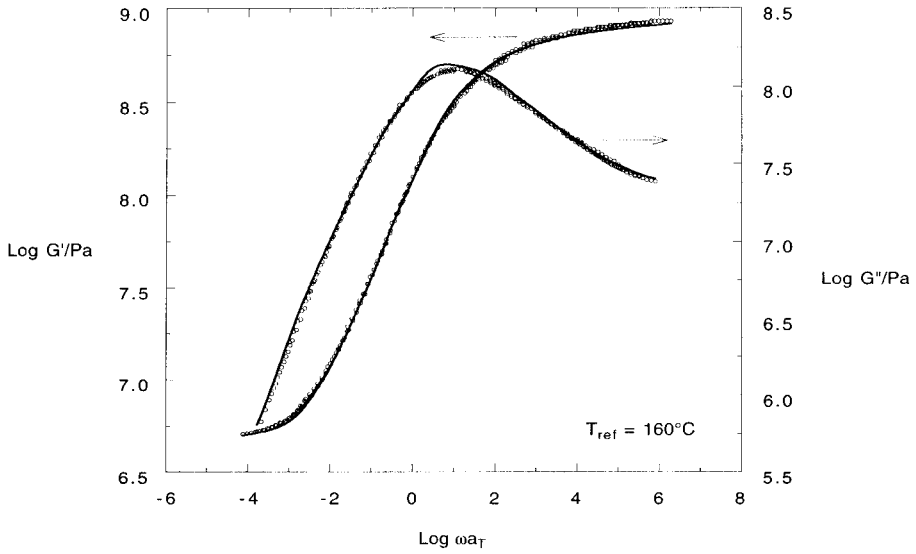

Figure 3 The reduced curves for the storage and loss moduli for the fully-cured material, both at a reference temperature of 160°C, are shown as data points. The lines are eqs. (1) and (2). The parameters used in the equations were obtained by simultaneously fitting the reduced curves for the storage modulus, loss modulus, and stress relaxation modulus (see Fig. 4) to eqs. (1), (2), and (3), respectively.

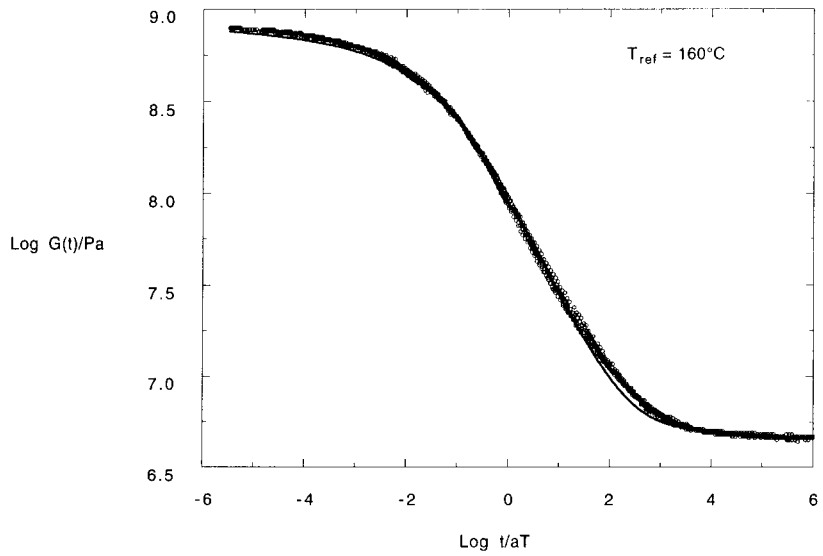

Figure 4 The reduced stress relaxation curve for the fully cured material at a reference temperature of 160°C, is shown as data points. The line is eq. (3). The parameters used in the equation were obtained by simultaneously fitting the reduced curves for the storage modulus, loss modulus, and stress relaxation modulus to eqs. (1), (2), and (3), respectively.

stress relaxation is shown in Figure 4. The three master curves were simultaneously fit to eq. (1), (2), and (3) using a least-squares regression to find the weighting factors for the relaxation times. Based on a χ^2 analysis, the average relative difference between the data and the fits is less than 3.3% for $G'(\omega)$, 5.2% for $G''(\omega)$, and is 5.8% for $G(t)$. The parameters G_g and G_r used to fit the master curves are shown in Table I along with their standard errors. The standard error for G_r was calculated from the scatter in the limiting long-time value obtained from stress relaxation measurements; the standard error in G_g was calculated assuming that the model parameters are independent. The relaxation times and corresponding weighting factors used in the fits are tabulated in Table II.

Table I Rubber and Glassy Moduli and Vogel Parameters Used to Fit the Viscoelastic Master Curves for the Fully Cured Material

Parameter	Value	Standard Error
G_g (Pa)	8.58×10^8	0.33×10^8
G_r (Pa)	4.63×10^6	0.05×10^6
C (K)	42,420	260
T_∞ (K)	0.0	1.4

Table II Relaxation Time Spectrum Used to Fit Viscoelastic Data at 160°C For the Fully Cured Material

g_i	$\log \tau_i$
0.0215	−7.0
0.0215	−6.5
0.0215	−6.0
0.0215	−5.5
0.0267	−5.0
0.0267	−4.5
0.0375	−4.0
0.0405	−3.5
0.0630	−3.0
0.0630	−2.5
0.1054	−2.0
0.1160	−1.5
0.1160	−1.0
0.1653	−0.5
0.0561	0.0
0.0561	0.5
0.0199	1.0
0.0119	1.5
0.0055	2.0
0.0028	2.5
0.0008	3.0
0.0002	3.5
0.0003	4.0
0.0003	5.0

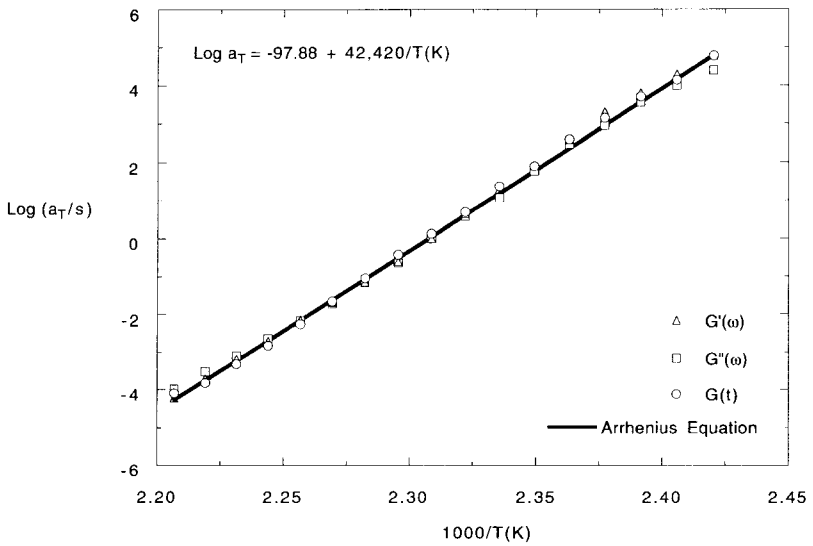

Figure 5 Logarithm of the shift factor vs $1/T$. The shift factors were obtained from shifting $G'(\omega)$ and $G''(\omega)$ data to obtain the reduced curves shown in Figure 3 and from shifting $G(t)$ data to obtain the reduced curve in Figure 4. The fit of the Arrhenius equation is shown.

The shift factors used to reduce the viscoelastic data are shown in Figure 5. The shift factors for all three viscoelastic functions agree indicating that the data are consistent. The temperature dependence is found to be Arrhenius; i.e., the Vogel temperature T_∞ is -273.2°C. The value of C and T_∞ (in eq. (12)) are given in Table I along with the standard errors obtained from the fit; the standard error reported is that obtained assuming that the two parameters are independent. From the value of C, an apparent activation energy of 353 ± 2 kJ/mol is calculated at T_g.

Relationship between T_g and Conversion

The T_g-conversion data obtained from DSC are needed to model the viscoelastic properties as a

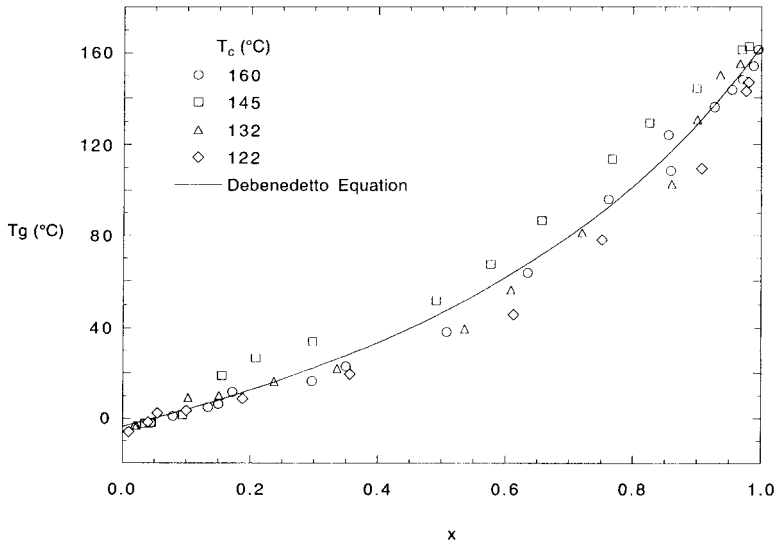

Figure 6 The relationship between T_g and conversion as measured by DSC is shown for four cure temperatures. The best fit of the Debenedetto equation (eq. (13)) is given by the line.

Table III Parameters for T_g Vs Conversion Relationship From DSC

Parameter	Value	Standard Error
T_{go} (°C)	−3.5	2.4
$T_{g\infty}$ (°C)	163.0	3.5
λ	0.43	0.04

function of conversion during cure since the shift factor $\log a_{T,x}$ depends on T_g (as in eq. (12)). The relationship between T_g and conversion is shown in Figure 6. Unlike many simpler epoxy systems, the T_g-conversion relationship from DSC appears to have a slight dependence on the cure temperature, perhaps due to the phase separation that occurs during cure for this epoxy system. The DeBendetto equation describes the DSC T_g-conversion relationship, with the parameter λ ranging from 0.28 to 0.66. The best fit of all the data gives $\lambda = 0.43$, with a standard error of 0.04. This value and the best fit values for T_{go} and $T_{g\infty}$ for all of the DSC data are shown in Table III.

Cure Kinetics

In order to model the evolution of the viscoelastic properties as a function of time during cure, we also need to know the cure kinetics. The cure kinetics of this epoxy system are assumed to be similar to that reported in the literature, i.e., first order in epoxy concentration, first order in cross-linker concentration, and autocatalytic.[19–26]

$$\frac{dx}{dt} = -k_{\text{eff}}(1 - x)(1/r - x)(x + b) \qquad (18)$$

where k_{eff} is the effective rate constant, r is the stoichiometric ratio of the limiting reagent to the excess reagent ($r < 1.0$), and b allows for the second-order reaction that initially starts the cure, which is presumably catalyzed by impurities. We allow for the assumption that the epoxy and cross-linker are not present in a stoichiometric ratio because industrial blends of epoxy and cross-linker are generally not stoichiometric. The rate constant k_{eff} is simply the Arrhenius temperature dependent rate constant k in the absence of diffusion control:

$$k = k_o e^{-(E/RT)} \qquad (19)$$

where E is the activation energy, R is the gas constant, and T is the absolute temperature. However, when the material vitrifies during cure, diffusion control dominates the reaction and the effective rate constant decreases. The effect of diffusion control is incorporated into the model of the cure kinetics following the methodology applied in other work[25–28] by allowing the time scale of the reaction (the reciprocal of the effective rate constant) to be the sum of the timescale for diffusion plus the time scale for chemical reaction in the absence of diffusion:

$$\frac{1}{k_{\text{eff}}} = \frac{1}{k} + \frac{1}{k_d} \qquad (20)$$

where k_d is assumed to follow the form of the Doolittle equation[29] using the "universal" WLF parameters[5]:

$$k_d = k_{do} e^{-(B/f)} \qquad (21)$$

$$f = (T_c - T_g)(4.8 \times 10^{-4}) + 0.025 \qquad (22)$$

where B is a constant and f is the free volume fraction that is considered per the above equation to depend on the distance $(T - T_g)$. The limiting value of f for $T \ll T_g$ is such that k_d goes to zero. Because we obtained relatively little data in the diffusion-controlled regime, we take B as 0.20 as was found in the modeling of other epoxy systems.[26] We note that we tried also using the viscoelastic shift factor to model k_d ($k_d = k_{d,\text{ref}}/a_{T,x}$, where $k_{d,\text{ref}}$ is the reciprocal time constant for diffusion at the reference temperature and $a_{T,x}$ is given by eq. (12)), but the fit was not as good as when using the "universal" WLF parameters.

There are five parameters that may be adjusted to fit the experimental data: k_o, E, r, b, and k_{do}. To determine these parameters, we used T_g versus time data rather than conversion versus time data because T_g is a more accurate and sensitive parameter for monitoring the reaction at high conversions due to the shape of the $T_g - x$ relationship[25,26] and because the mechanical properties are more sensitive to T_g than to conversion—see the equations for $\log a_{T,x}$ and G_r that depend explicitly on T_g and x, respectively (eqs. (11) and (4–6)). In fact, we note that diffusion control after vitrification did not need to be invoked to obtain a good fit of the conversion data, whereas diffusion control did need to be invoked to fit the same data when T_g was used as the

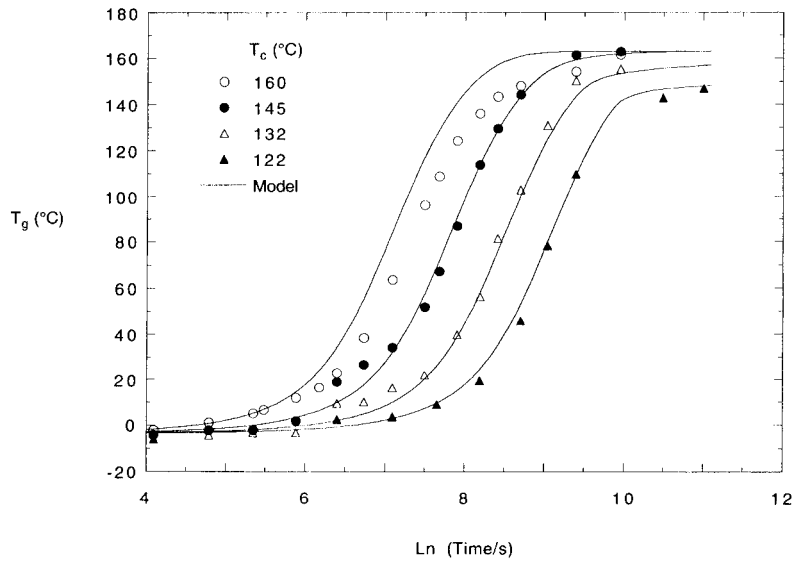

Figure 7 The evolution of T_g with time of cure at four isothermal curing temperatures is shown. The lines give the fit to the second-order autocatalytic kinetic model with parameters listed in Table IV.

measure of the reaction due to the high sensitivity of T_g to changes in conversion at high conversions.

The fit of the model of the cure kinetics to the experimental DSC T_g versus logarithmic time data are shown in Figure 7. The agreement is very good at the lowest three cure temperatures (where the fitting was done) and in the diffusion-controlled regime. The parameters used in the fit and their standard errors obtained assuming parameters are independent are given in Table IV. The stoichiometric ratio of reactants is found to be 0.83 ± 0.04 from the fit of the data to eqs. (18) through (22). The component in excess is not known.

Evolution of Dynamic Mechanical Properties During Cure

The evolution of the storage modulus at 1 Hz as predicted by the thermo-viscoelastic model is shown as a function of conversion in Figure 8 for cure temperatures of 145, 160, 170, and 180°C. The response is only shown after gelation (which occurs at approximately 63% conversion for a stoichiometric ratio of 0.83) because prior to gelation, the rubbery modulus is zero. At gelation, the cross-link density begins to increase, and hence the rubbery modulus and $G'(\omega)$ also begin to increase. For the lowest cure temperatures, there is also a sharp increase in the storage modulus at higher conversions due to vitrification.

To verify the model, we compared the thermo-viscoelastic model to experimental storage modulus data that were obtained as a function of time during isothermal cure at four curing temperatures (following a temperature ramp to the cure temperature as described in the experimental section). Using the cure kinetic parameters in Table IV, we transformed the conversion axis of Figure 8 to a time axis in order to do the comparison. The evolution of $G'(\omega = 1$ Hz) as a function of time at the four temperatures studied is shown in Figures 9 through 12. The open symbols are the experimental data and the solid lines in the figures represent the calculation from our thermo-viscoelastic model with no adjustments made except that the time to gelation was set at that observed experimentally. (We integrated the cure kinetic model equation 18 from $x = x_{gel} = 0.633$ at $t = t_{gel}$, with the time to gelation taken as the time at which $G'(\omega = 1$ Hz) is observed experi-

Table IV Parameters Used in the Model of the Cure Kinetics

Parameter	Value	Standard Error
k_o (s^{-1})	3.0×10^6	0.04×10^6
b	0.124	0.004
r	1.20	0.05
E/R (K)	8988	5
k_{do} (s^{-1})	5566	3351

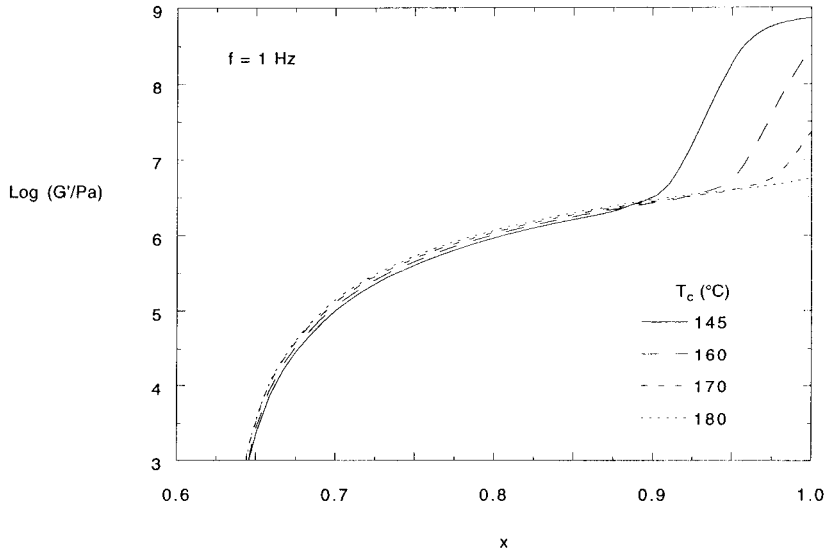

Figure 8 The calculated evolution of the storage modulus measured at 1 Hz as a function of conversion for four cure temperatures.

mentally to become finite. This procedure avoids making assumptions about the cure kinetics and reaction exotherm, the latter of which will be important primarily at low conversions where the reaction rate is high.) All model parameters used in the calculations were based on the experimental master curves of the "fully cured" material, the temperature dependence of the shift factors for the "fully cured" material, and the T_g-conversion relationship. The model, with no adjustable parameters, quantitatively captures very well the evolution of the dynamic mechanical response of this epoxy during cure. These results demonstrate that the current model, which is based on the principles of time-temperature and time-cross-link density superposition along with concepts of rubber elasticity, provides a powerful tool for modeling the evolution of viscoelastic properties of thermosetting materials during cure.

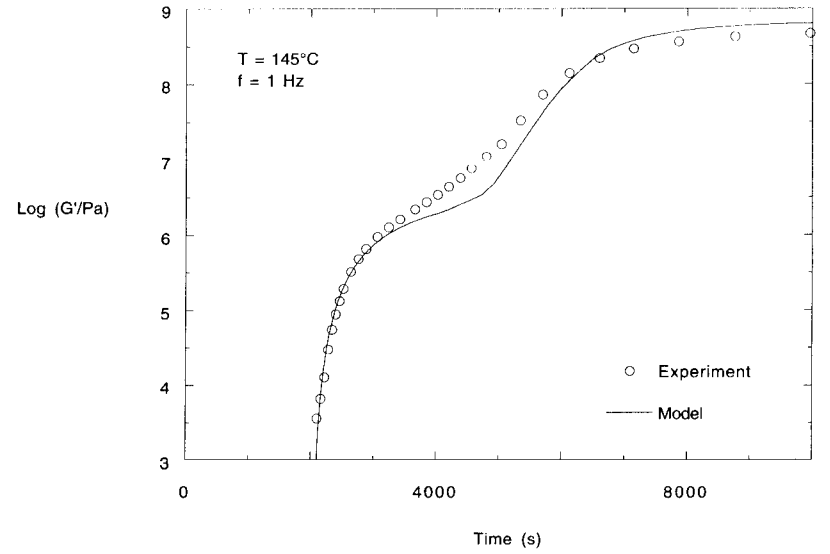

Figure 9 The evolution of the storage modulus during isothermal cure at 145°C is given by the data points. The line shows the model calculation.

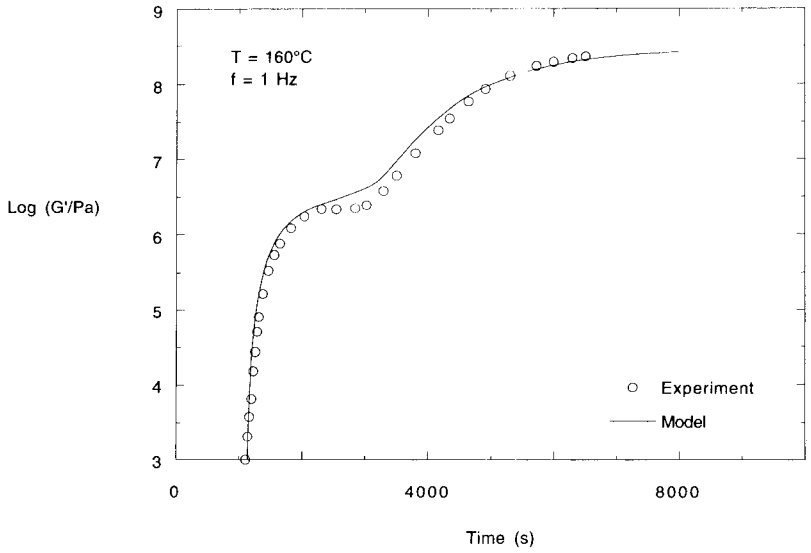

Figure 10 The evolution of the storage modulus during isothermal cure at 160°C is given by the data points. The line shows the model calculation.

DISCUSSION

We assumed in our model that time-temperature-cross-link density superposition holds. In other words, the shape of the retardation spectrum is assumed to not vary with temperature or conversion (cross-link density) but is simply shifted along the time axis. The assumption of thermorheological simplicity, that the spectrum shape does not change with temperature, is thought to be reasonable based on the many works that show that this is approximately if not completely valid, including those cited in our references.

For time-conversion superposition, on the other hand, Plazek and Chay[12] show using their model epoxy system that the retardation spectrum narrows with increasing degree of cure after gelation because as the cross-link density increases, the molecular weight between cross-links decreases, and the long-time mechanisms disap-

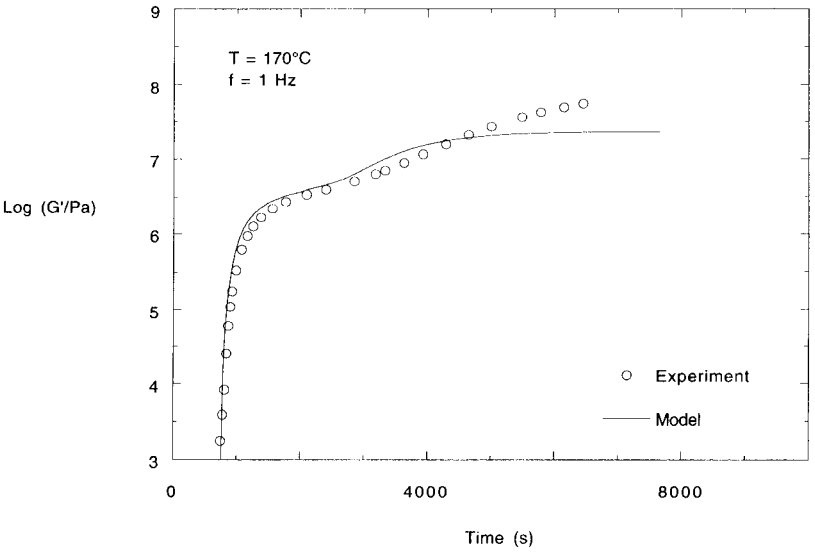

Figure 11 The evolution of the storage modulus during isothermal cure at 170°C is given by the data points. The line shows the model calculation.

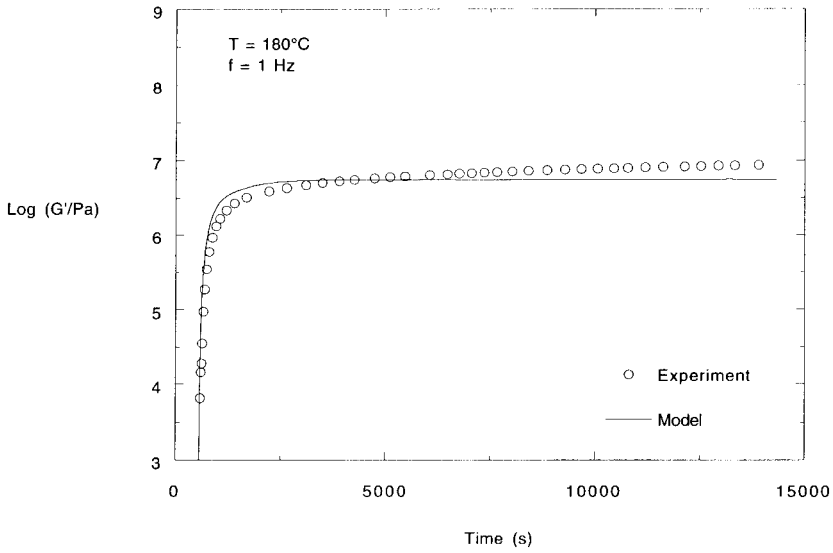

Figure 12 The evolution of the storage modulus during isothermal cure at 180°C is given by the data points. The line shows the model calculation.

pear. Hence, the spectra for materials of different degrees of cure do not superpose in the terminal region of response. However, the spectra do superpose at short times and through the softening dispersion independent of degree of cure. We expect that these short- and medium-range relaxations, rather than the terminal relaxations, are those that dominate the viscoelastic response during the vitrification process that we are modeling. Hence, although the assumption of a structural-rheological simplicity is not expected to be strictly valid, it appears to be a good approximation for modeling the evolution of viscoelastic properties during cure after gelation.

The model is very sensitive to the cure kinetics. For example, the deviation between the calculation and the data for cure at 170°C, shown in Figure 11, can be virtually eliminated by assuming that the cure was slower and took place at 167°C. The result suggests that the T_g-conversion relationship and/or the model of the cure kinetics, shown in Figures 6 and 7, may be more complicated than assumed, as previously discussed. The result also emphasizes the necessity for accurate kinetic models in order to obtain an accurate description of the evolution of mechanical properties.

CONCLUSIONS

We have constructed a model for the evolution of the shear modulus of a commercial epoxy resin during cure. The model incorporates time-temperature superposition and time-cross-link density superposition principles along with concepts of rubber elasticity in thermosets. The model parameters are obtained from viscoelastic measurements for the fully cured resin and a recursive model for the evolution of the rubbery modulus of the network. Input of the cure kinetics from a conventional model permits calculation of the evolution of the shear storage modulus given the cure temperature history. The behavior of $G'(\omega = 1$ Hz) from the model agreed well with the experiments from the point of gelation through vitrification for four isothermal curing temperatures with no adjustable parameters.

Partial support of this project by ACS PRF Grant No. 32555 AC7 and by General Electric Company is gratefully acknowledged. We also thank Hexcel Corporation for providing material. Major portions of this work were performed at the University of Pittsburgh and at the National Institute of Standards and Technology.

REFERENCES

1. Gillham, J. K. Polym Eng Sci 1986, 26(20), 1429.
2. Enns, J. B.; Gillham, J. K. J Appl Polym Sci 1983, 28, 2567.
3. Leaderman, H. Elastic and Creep Properties of Filamentous Materials, Textile Foundation: Washington, D.C., 1943.
4. Ferry, J. D. Viscoelastic Properties of Polymers; John Wiley and Sons: New York, 1980.

5. Williams, M. L.; Landell, R. F.; Ferry, J. D. J Am Chem Soc 1955, 77, 3701.
6. Vogel, H. Phys Z 1921, 22, 645.
7. Kitoh, M.; Suzuki, K. Kobunshi Ronbunshu, Eng Ed 1975, 4(3), 184.
8. Suzuki, K.; Miyano, Y.; Kunio, T. J Appl Polym Sci 1977, 21, 3367.
9. Kitoh, M.; Suzuki, K. Kobunshi Ronbunshu, Eng Ed 1976, 5(1), 26.
10. Plazek, D. J. J Polym Sci: Part A-2 1966, 4, 745.
11. Lee, A.; McKenna, G. B. Polymer 1988, 29, 1812.
12. Plazek, D. J.; Chay, I.-C. J Polym Sci: Part B: Polym Phys 1991, 29, 17.
13. Miller, D. R.; Macosko, C. W. Macromolecules 1976, 9(2), 206.
14. Aronhime, M. T.; Gillham, J. K. J Coat Tech 1984, 56(718), 35.
15. Mijovic, J.; Wijaya, J. Macromolecules 1990, 23, 3671.
16. Hale, A.; Macosko, C. W.; Bair, H. E. Macromolecules 1991, 24, 2610.
17. Nelson, L. E. J Macromol Sci Rev Macromol Chem 1969, C3, 69.
18. Struik, L. C. E. Physical Aging in Amorphous Polymers and Other Materials; Elsevier Press: Amsterdam, 1978.
19. Ricardo, C. C.; Adabo, H. E.; Williams, R. J. J. J Appl Polym Sci 1984, 29, 2481.
20. Horie, K.; Hiura, H.; Sawada, M.; Mita, I.; Kambe, H. J Polym Sci 1970, A-1, 8, 1357.
21. Chiao, L. Macromolecules 1990, 23, 1286.
22. Matejka, L.; Dusek, K. Macromolecules 1989, 22, 2911.
23. Chern, C.-S.; Poehlein, G. W. Polym Eng Sci 1987, 27(11), 788.
24. Titier, C.; Pascault, J-P.; Taha, M.; Rozenberg, B. J Polym Sci: Part A: Polym Chem 1995, 33, 175.
25. Wisanrakkit, G.; Gillham, J. K. J Coat Tech 1990, 62(783), 35.
26. Simon, S. L.; Gillham, J. K. J Appl Polym Sci 1992, 46, 1245.
27. Matsuoka, S.; Quan, X.; Bair, H. E.; Boyle, D. J. Macromolecules 1989, 22, 4093.
28. Sanford, W. M.; McCullough, R. L. J Polym Sci: B: Polym Phys 1990, 28, 973.
29. Doolittle, A. K. J Appl Phys 1951, 22, 1471.